Evaluation of Existing Viscosity Data and Models and Developments of New Viscosity Model for Fully Liquid Slag in the SiO_2-Al_2O_3-CaO-MgO System

CHEN HAN, MAO CHEN, WEIDONG ZHANG, ZHIXING ZHAO, TIM EVANS, and BAOJUN ZHAO

Metallurgical properties of slag are determined to a great extent by its viscosity. High-temperature viscosity measurements are time-consuming and expensive. It is necessary to develop an accurate viscosity model for blast furnace slag in the SiO_2-Al_2O_3-CaO-MgO system using reliable viscosity data. This paper describes a systemic evaluation procedure to determine the viscosity data to be used for model development. 1780 viscosity data from 10 to 65 wt pct SiO_2, 3.5 to 40 wt pct Al_2O_3, 2 to 60 wt pct CaO, and 2 to 38 wt pct MgO in the SiO_2-Al_2O_3-CaO-MgO system have been accepted for model evaluation after critical reviews. The existing 14 viscosity models in SiO_2-Al_2O_3-CaO-MgO system is also reviewed and evaluated. Based on the structure of alumina-silicate slag and evaluated viscosity data, a new viscosity model has been proposed for the system SiO_2-Al_2O_3-CaO-MgO. A new term "probability," based on the basic oxide and electronegativity, is introduced to calculate the integral activation energy of slag. The model has been evaluated and compared with existing viscosity models in three different composition ranges in SiO_2-Al_2O_3-CaO-MgO system for different applications. The new model reports an outstanding agreement between predictions and experimental data. The industrial implications of the new model have also been discussed in ironmaking and steelmaking processes.

DOI: 10.1007/s11663-016-0744-4

I. INTRODUCTION

VISCOSITY is one of the important physicochemical properties of slags in metallurgical process, which significantly impact on operation and fuel usage efficiency.[1] In ironmaking and steelmaking industry, SiO_2-Al_2O_3-CaO-MgO system is one of the major systems for blast furnace (BF) slags and steelmaking slags.[2–4] The approximate composition ranges of typical BF and ladle slags are shown in Table I. It can be seen that ladle slags have higher CaO/SiO_2 and Al_2O_3 than BF slags.[5]

In ironmaking and steelmaking process, proper viscosity of slag leads to (a) fluently flowing in tapping process, (b) efficient desulphurization, (c) controllable accretion formation on the furnace wall, (d) easy separation from hot metal and coke (Ironmaking),[1] and (e) well dispersion of inclusion (Steelmaking).[5] However, high-temperature viscosity measurements are complex, fallibly techniques, cost- and time-consuming. It is necessary to establish a viscosity model to provide reliable information for process optimization.

Successful development of a viscosity model always depends on large numbers of reliable data. The quality and quantity of the data directly influence the viscosity model performance. Abundant viscosity measurements in the SiO_2-Al_2O_3-CaO-MgO system have been carried out at wide ranges of compositions and temperatures.[6–42] A critical and systematic examination of the experimental measurements is essential to adopt reliable data for the development of viscosity model.

The present study aims to establish an accurate viscosity model in SiO_2- Al_2O_3-CaO-MgO quaternary system. A systemic evaluation procedure to select valuable viscosity data were firstly performed, followed by reviewing and evaluating the available viscosity models in SiO_2-Al_2O_3-CaO-MgO system. Using the accepted data above, a new viscosity model is proposed for SiO_2-Al_2O_3-CaO-MgO system and the performance of this model is compared with other existing models.

II. REVIEW OF EXPERIMENTAL VISCOSITY DATA

3135 viscosity data in the SiO_2-Al_2O_3-CaO-MgO system have been critically reviewed from 37 publications.[6–42] The measurements have covered compositions of 10 to 67 wt pct SiO_2, 1 to 40 wt pct Al_2O_3, 1 to 60 wt pct CaO, 1 to 38 wt pct MgO, and temperatures

CHEN HAN, Ph.D. Student, MAO CHEN, Postdoctoral Research Fellow, and BAOJUN ZHAO, Codelco-Fangyuan Professor, are with the School of Chemical Engineering, the University of Queensland, Australia. Contact e-mail: baojun@uq.edu.au WEIDONG ZHANG and ZHIXING ZHAO, Professors of Engineering, are with Shougang Research Institute of Technology, Beijing, China. TIM EVANS, Principal Engineer, is with Rio Tinto Iron Ore, Sydney, Australia.

Manuscript submitted March 12, 2016.
Article published online July 11, 2016.

Table I. Typical Composition of BF Slag and Ladle Slag[1,2,5]

Composition (Wt Pct)	BF Slag	Ladle Slag
SiO_2	30 to 40	10 to 25
Al_2O_3	10 to 15	20 to 30
CaO	35 to 45	40 to 50
MgO	5 to 10	5 to 10
Basicity (CaO/SiO_2)	1.1 to 1.3	2 to 3

between 1623 K and 1823 K (1350 °C to 1550 °C). Measurement of slag viscosity at high temperatures is difficult and has potential for large uncertainties in the results. Hence, three sequential steps are used to evaluate the experimental data:

- Review experimental techniques.
- Check data self-consistency.
- Cross-reference comparison.

A. *Experimental Techniques in Viscosity Measurements*

The improper selection and setting of viscometer will increase measurement uncertainty. Three types of viscometer have been used: rotational viscometer (28 publications),[6–33] oscillation plate viscometer (7 publications),[34–40] and falling-ball viscometer (2 publications).[41,42] It is widely accepted that the rotational viscometer is a more reliable viscosity measurement technique compared to others.[43] Still, few researchers reported detailed setting parameters: spindle weight, distances between the spindle and crucible, and thermal expansion that have studied and reported as uncertainty factor by the present authors.[6] The oscillating plate viscometer suits better for low viscosity within the range of 10^{-5} to 10^{-2} Pa s, such as pure liquid metal system.[44] For falling-ball viscometer, it has been found that the thermal expansion of the sensor (ball) significantly increases viscosity measurement uncertainty, ranges from 1 to 100 Pa s, which depends on temperature and falling-ball material.[45] The viscosities measured by falling-ball viscometer were rejected because of large uncertainty. The measurements by oscillating plate and rotational viscometer are reviewed as follows.

Mill *et al.*[43] reported that improper selection of container/sensor materials can cause significant uncertainty (>50 pct) in viscosity measurement. At high temperatures, the aggressive molten slags may react with the container and sensor materials leading to changes in slag composition or container/sensor geometry. Pt, Pt/Rh alloy, Fe, Mo, and graphite are major materials used for containers and sensors in the reviewed studies.[6–42] Most of researchers used Ar,[6,7,10,11,16–18,20–22,25–27,29–31,33] N_2,[9] or CO[8] gas to prevent potential oxidation of crucible/spindle. Bockris *et al.*[46] reported that graphite material may reduce SiO_2 and form SiC at high temperature, which will change slag composition and contribute to experimental uncertainties. The reaction initiated above 1793 K (1520 °C), which was estimated by FactSage 6.2.[47] The viscosity data from graphite container/sensor were carefully reviewed, and high-temperature data were found not reliable and rejected (>1793 K) (1520 °C). When Mo was used for spindle and crucible, it could be oxidized if the system was not sealed properly. The resulted MoO_3 would dissolve into the slag and affect the viscosity. For most of the experiments, the conditions were not reported in details and possible oxidation of Mo was not considered. This criterion is not used in the present study. Pt sensor/container were used in air for viscosity measurements.[28,35–37,41] Despite the chemical reactions, the geometry of container/sensor can be physically changed at high temperatures due to thermal expansion and softening. The hardness of metal keeps reducing when temperature approaches the melting point. The melting temperatures of pure Fe and Pt are 1811 K and 2031 K (1538 °C and 1798 °C), respectively. Therefore, the viscosity measurements taken under improper container/sensor materials and temperature are not reliable and will not be accepted for model evaluation.

In 37 publications, three publications[18,38,39] reported nonequilibrium viscosity measurements, in which the viscosity data were recorded during continuous-cooling process. The viscosity and internal structure of the molten slag do not correspond to the recorded temperature if the time is not enough for equilibrium. For the same slag, the viscosity measured on continuous-cooling is shown to be lower than the viscosity measured at steady condition at the same temperature.[48] Therefore, nonequilibrium viscosity measurements are not accepted in the database for viscosity model.

Slag compositions, presence of solid, and container/sensor geometry changes can be examined by postexperimental technology. However, none of the slag samples was quenched after viscosity measurements in 36 publications,[7–42] except the measurements by present authors.[6] The EDS, XRF, and ICP analyses were often used to determine slag composition. The techniques of postexperimental analysis are summarized in Table II.

In summary, from 37 publications, the reported methodology is not sufficient to filter out the reliable viscosity data. Therefore, self- and cross-consistency of viscosity data should be checked.

B. *Data Consistency*

Liquidus temperature of the slag is an important indicator to discover inappropriate measurements of the viscosity. The phase diagrams of the system SiO_2-Al_2O_3-CaO-MgO[43] have been reported and they are used together with FactSage 6.2[47] to predict the liquidus temperature of slag. The viscosity of bulk slag with solid precipitations is much higher than that in fully liquid condition. For example, it can be seen from Figure 1 that the viscosities measured at lower temperatures of two sets data are much higher than the rest of data in the same set at high temperatures. As indicated in the figure, these high viscosities were measured at the temperatures below their liquidus. The last point in each set is rejected due to the presence of solid phase.

It is well known that slag viscosity and temperature follows the Arrhenius-type equation[49]:

Table II. Summary of Viscosity Data for the System SiO_2-Al_2O_3-CaO-MgO,[6–42]

Sources	Method	Atmosphere	Container	Sensor	Temperature [K (°C)]	Post Experiment Techniques	Viscosity (Pa s)	Total No. of Data	No. of Accepted Data
Chen *et al.*[6]	RB	Ar	Mo	Mo	1673 to 1823 (1400 to 1550)	EPMA	0.2 to 1.2	20	20
Forsbacka *et al.*[7]	RB	Ar + 5 pctCO	Mo	Mo	1853 to 2033 (1580 to 1750)	EDS	0.08 to 0.6	50	50
Gao *et al.*[8]	RB	CO	C	Mo	1723 to 1823 (1450 to 1550)	XRD	0.33 to 2.21	36	36
Gul'tyai[9]	RB	N_2	C	C	1523 to 1823 (1250 to 1550)	N/A	0.2 to 10	633	234
Gupta and Seshadri[10]	RB	Ar	C	C	1673 to 1823 (1400 to 1550)	N/A	0.28 to 3.24	493	245
Han *et al.*[11]	RB	Ar	C	Pt-10Rh	1573 to 1873 (1300 to 1500)	N/A	0.3 to 0.8	5	3
Hofmann[12]	RB	Air	Pt	Pt	1723 to 1873 (1450 to 1600)	EDS	0.1 to 3	59	41
Hofmann[13]	RB	n/a	C	N/A	1673 to 1823 (1400 to 1550)	EDS	0.11 to 2.17	24	4
Johannsen and Brunion[14]	RB	n/a	Pt/20Rh	Pt/20Rh	1523 to 1723 (1250 to 1450)	EDS	20 to 900	13	4
Kawai[15]	RB	n/a	C	C	1773 to 1873 (1500 to 1600)	N/A	0.09 to 90	69	19
Kim *et al.*[16]	RB	Ar	C	N/A	1673 to 1823 (1400 to 1550)	XRF	0.136 to 2.41	13	8
Kim *et al.*[17]	RB	Ar	Pt-10Rh	Pt-10Rh	1698 to 1773 (1425 to 1500)	N/A	0.04 to 5.1	79	61
Kim and Seo[18]	RB	Ar	Pt/10Rh	Pt/10Rh	1723 to 1773 (1450 to 1500)	ICP	0.3 to 0.5	122	0
Koshida *et al.*[19]	RB	N/a	N/A	N/A	1633 to 1773 (1360 to 1500)	EDS	0.03 to 3.81	32	22
Li and Ning[20]	RB	Ar	Mo	Mo	1673 to 1823 (1400 to 1550)	N/A	0.1 to 1	104	104
Lee *et al.*[21]	RB	Ar	Pt/10Rh	Fe	1673 to 1723 (1400 to 1450)	N/A	0.3 to 1	14	13
Lee *et al.*[22]	RB	Ar	Pt/10Rh	Fe	1673 to 1723 (1400 to 1450)	XRF	0.3 to 0.9	12	9
Mishra *et al.*[23]	RB	N_2	C	n/a	1623 to 1848 (1350 to 1575)	N/A	0.1 to 4.6	179	81
Muratov and Kulikov[24]	RB	n/a	Mo	Mo	1573 to 1923 (1300 to 1650)	N/A	0.2 to 5	57	20
Nakamoto *et al.*[25]	RB	Ar	Fe	Fe	1523 to 1723 (1250 to 1450)	EDS	0.29 to 2.89	6	6
Park *et al.*[26]	RB	Ar	Pt-10Rh	Pt-10Rh	1598 to 1773 (1325 to 1500)	XRD	0.15-0.8	16	16
Saito *et al.*[27]	RB	Ar	Pt-20Rh	Pt-20Rh	1673 to 1873 (1400 to 1600)	N/A	0.1 to 1.3	20	20
Scarfe *et al.*[28]	RB	Air	Pt	Pt/10Rh	1448 to 1873 (1175 to 1600)	N/A	0.4 to 100	64	49
Shankar *et al.*[29]	RB	Ar	Mo	Mo	1673 to 1873 (1400 to 1600)	ICP	0.16 to 2.55	30	29
Song *et al.*[30]	RB	Ar	Mo	Mo	1748 to 1903 (1475 to 1630)	EDS	0.12 to 0.56	63	56
Tang *et al.*[31]	RB	Ar	Mo	Mo	1538-1798 (1265-1525)	N/A	0.31-10.03	105	101
Vyatkin *et al.*[32]	RB	n/a	C	C	1573-1773 (1300-1500)	N/A	0.3-5	15	15
Yao *et al.*[33]	RB	Ar	C	Mo	1673-1823 (1400-1550)	XRF	0.1-1	48	48
Kita *et al.*[34]	OP	n/a	Pt	Pt	1523-1773 (1250-1500)	EDS	0.6-10	12	12
Machin and Hanna[35]	OP	Air	Pt	Pt-alloy	1523-1773 (1250-1500)	X-ray	0.2-2.83	562	390
Machin and Yee[36]	OP	Air	Pt	Pt-alloy	1523-1773 (1250-1500)	X-ray	1-30		
Machin *et al.*[37]	OP	Air	Pt	Pt-alloy	1523-1773 (1250-1500)	X-ray	0.2-60		
Sheludyakov *et al.*[38]	OP	n/a	Pt	Pt	1513-1683 (1240-1410)	N/A	Jan-40	18	0
Tsybulnikov *et al.*[39]	OP	n/a	Mo	Mo	1773-1973 (1500-1700)	N/A	0.1-0.4	14	0
Yakushev *et al.*[40]	OP	n/a	Mo	Mo	1733-1998 (1460-1725)	N/A	0.08-0.7	92	64
Kato and Minowa[41]	FB	Air	Pt	Pt	1618-1748 (1345-1475)	N/A	0.3-2	10	0
Taniguchi[42]	FB	n/a	Pt	Pt	1373-1923 (1100-1650)	N/A	0.4-400	46	0

RB: rotational bob viscometer; OP: oscillation plate viscometer; FB: falling-ball viscometer.

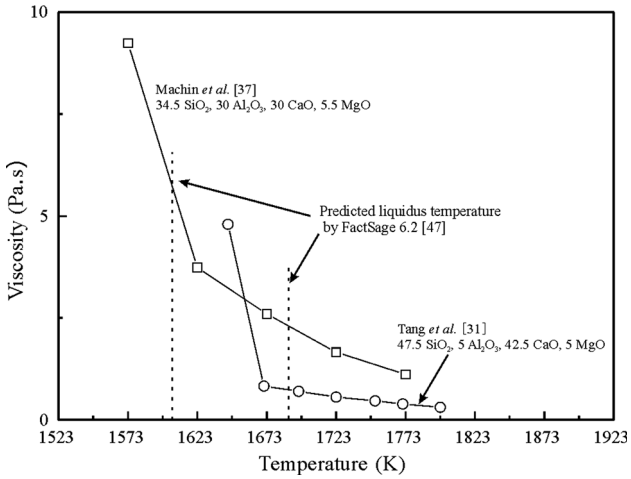

Fig. 1—Examples showing viscosity measured by Machin *et al.*[37] and Tang *et al.*[31] below liquidus predicted by FactSage 6.2.[47]

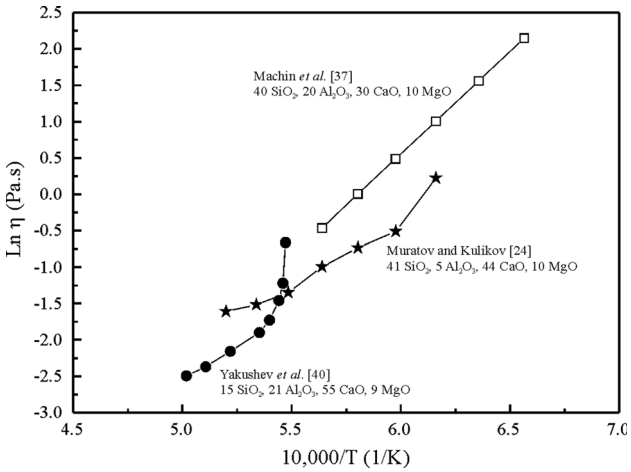

Fig. 2—Linearity of three examples by Muratov and Kulikov,[24] Machin *et al.*[35] and Yakushev *et al.*[40]

$$\ln \eta = \ln A + \frac{E}{T}, \qquad [1]$$

where η is viscosity in Pa s, A is the pre-exponential factor, E is the activation energy in J/mol, and T is the absolute temperature in K.

According to Eq. [1], the natural logarithm of viscosity has a linear correlation to reciprocal of absolute temperature. Figure 2 shows examples of viscosity measurements with high and low consistencies. The data from Machin *et al.*[37] show a good linear relationship. In comparison, the data from Muratov and Kulikov[24] and Yakushev *et al.*[40] have a low reliability and they are excluded from the database. In Yakushev *et al.*'s data,[40] three data points at high temperatures increased dramatically indicating the viscosities were measured below liquidus. Due to insufficient information of postexperiment analysis from published papers, the reasons for other nonlinear results are not clear. Data linearity is a good indication to evaluate the measurements reliability in the absence of enough experimental conditions.

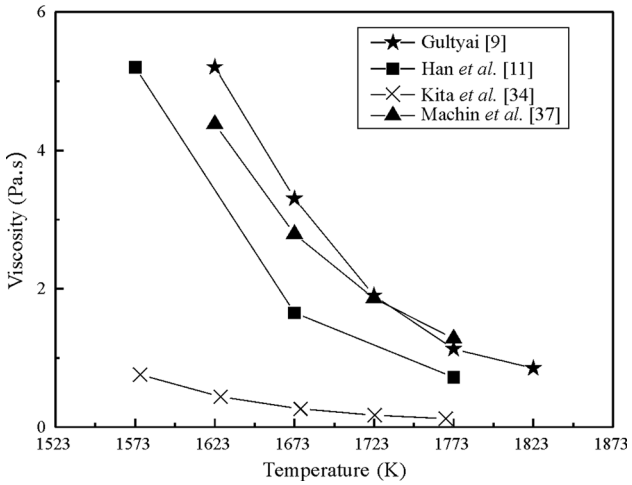

Fig. 3—Four sets viscosity measurement at 45 wt pct SiO_2, 15 wt pct Al_2O_3, 30 wt pct CaO, and 10 wt pct MgO by Gultyai,[9] Han *et al.*,[11] Kita *et al.*,[34] and Machin *et al.*[36]

C. *Cross-Reference Comparison*

The viscosities measured from different researchers at close compositions were carefully compared to cross check the reliability of the data. As shown in Figure 3, there were four sets of viscosity measurements[9,11,34,37] in the same composition and three sets of data[9,11,37] are close. Data from Kita *et al.*[34] are excluded from the database as they are significantly different from others.

In case the available viscosity data are not consistent and the information reported is not enough for the evaluation, the viscosities at this composition were measured by the present authors using a recently developed technique at the University of Queensland. Figure 4 is an example, where it can be seen that the results of Park *et al.*[26] are confirmed by the authors' measurements and Kim *et al.*'s[16] data are not accepted. The methodology was described in details in a previous publication.[6] The main feature of this technique is the possibility of quenching the slag sample immediately after the viscosity measurement. Electron probe X-ray microanalysis (EPMA) with wave spectrometers was used for microstructural and elemental analyses of the quenched samples. In addition, the possible errors associated with the high-temperature viscosity measurements have been analyzed and significantly minimized, which include effects of bob weight, distances to crucible, and thermal expansion during rotational viscometer measurements.[6]

The experimental conditions on high-temperature viscosity measurements have been critically reviewed and summarized from 37 publications.[6–42] As shown in Table II, the data measured in graphite crucible, such as Gualityi[9] and Gupta and Seshadri,[10] were mostly rejected. The data of three authors, Kim and Seo,[18] Sheludyakov *et al.*,[38] and Tsybulnikov *et al.*[39] were fully rejected because measurements were carried out at

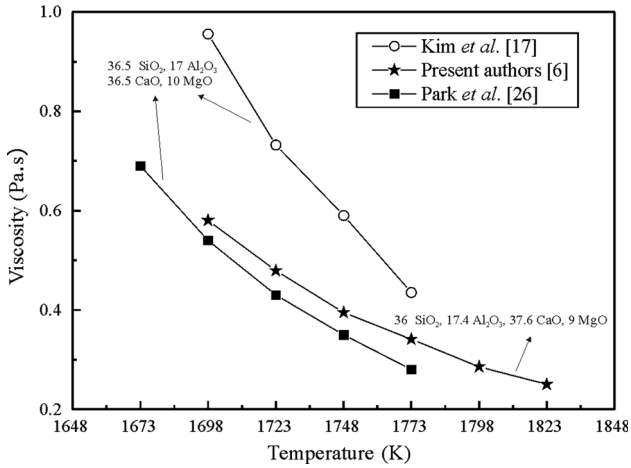

Fig. 4—Comparison of viscosity data by the present authors,[6] Kim *et al.*,[16] and Park *et al.*[26]

nonequilibrium condition. The viscosity data of Kato and Minowa[41] and Taniguchi[42] were also fully rejected because of large uncertainty at the falling-ball viscosmeter. Around one-third of Machin *et al.* 's[35–37] data were rejected, due to most of measuring temperatures were below liquidus temperatures of the slags. In summary, 1780 viscosity measurements from 10 to 65 wt pct SiO_2, 3.5 to 40 wt pct Al_2O_3, 2 to 60 wt pct CaO, and 2 to 38 wt pct MgO were accepted and utilized for viscosity model development in SiO_2-Al_2O_3-CaO-MgO system.

III. REVIEW OF VISCOSITY MODELS RELEVANT TO BF SLAGS

Abundant viscosity models related to SiO_2-Al_2O_3-CaO-MgO slags have been proposed in last decades[20,51–64] that correlate slag viscosity as a function of temperature and bulk composition. The parameters of mathematical equations were calculated from the physical properties of slag, for example, optical basicity and viscosity. In the present study, 14 existing[51–64] viscosity models relevant to SiO_2-Al_2O_3-CaO-MgO system are reviewed and evaluated using the accepted viscosity database from previous section.

A. *Features of the Existing Viscosity Model*

It is widely accepted that molten slag viscosity is determined by its internal structure. In SiO_2-Al_2O_3-CaO-MgO system, $(SiO_4)^{4-}$ tetrahedral forms the slag network, hence increases viscosity. Mg^{2+} and Ca^{2+} perform as network modifiers to reduce the slag viscosity. Al^{3+} can form $(AlO_4)^{5-}$ tetrahedral structure similar to $(SiO_4)^{4-}$ (network former). However, $(AlO_4)^{5-}$ requires Mg and Ca cations to balance the electrical charge. If amount of Ca and Mg cations are insufficient, Al^{3+} behaves as network modifier (same as Mg^{2+} and Ca^{2+}).[50]

The reviewed models can be categorized based on model structure, parameters, and consideration of the silicate structures. In different stages of the model developments, the understanding of alumina-silicate structure was different:

(I) Al_2O_3 as an amorphous oxide was not considered in the model development, such as Gan and Lai's[58] model.
(II) Al_2O_3 was considered as network former and introduced into the viscosity model. This includes the models of Urbain,[51] Riboud *et al.*,[52] Iida *et al.*,[53] Mill and Sridhar,[54] Shankar,[55] Ray and Pal,[56] Hu *et al.*,[57] Tang *et al.*,[59] Li *et al.*,[20] Suzuki and Jak,[60] and FactSage.[61,62]
(III) If basic oxides, *e.g.*, CaO and MgO are insufficient, the excess Al_2O_3 will behave as basic oxides. This was considered by the models of Shu[63] and Zhang *et al.*[64]

Researches established the viscosity models through different mathematical equations. The most popular equation was Arrhenius-type equation, which was utilized by Li *et al.*,[20] Urbain,[51] Riboud *et al.*,[52] Mill and Sridhar,[54] Shankar,[55] Ray and Pal,[56] Hu *et al.*,[57] FactSage,[61,62] Shu,[63] and Zhang *et al.*[64]:

$$\eta = A \times T^X \times e^{\frac{E_A}{RT}}, \quad [2]$$

where η is viscosity in Pa s, T is temperature in K, E_A is the slag activation energy in J/mol, A is pre-exponential factor, R is gas constant [8.314 J/(mol K)], X can be 0, 0.5, and 1 from different researchers.

Vogel–Fulcher–Tammann (VFT) as a classic equation for glass-forming liquid (Eq. [3]) was firstly proposed by Gan *et al.*[58] to predict slag viscosity of molten slag of SiO_2-Al_2O_3-CaO-MgO system:

$$\log(\eta) = A + \frac{B}{T - C}, \quad [3]$$

where η is viscosity in Pa s, T is temperature in K, and A, B, C are model parameters.

Iida *et al.*[53] and Tang *et al.*[59] proposed their own equations for viscosity prediction, which are shown in Eqs. [4] and [5], respectively.

$$\eta = A \times \eta_0 \times \frac{E}{B_i}, \quad [4]$$

where η is viscosity in Pa s, A and E are model parameters, η_0 is the viscosity of nonnetwork forming melts, and B_i is slag basicity determined using Iida equation.[53]

$$\log(\eta) = -8.4 - \frac{43.63}{3.75 + \left(\frac{\mathrm{NBO}}{T}\right)} + \frac{150450}{3.75 + \left(\frac{\mathrm{NBO}}{T}\right)} \times \frac{1}{T}, \quad [5]$$

where η is viscosity in Pa s, T is temperature in K, and NBO/T is defined as the ratio of nonbridging oxygen to total silicate ion.

Researchers proposed different mathematical formulas to correlate the slag structures with compositions. Urbain[51] firstly used weight ratio of $(W_{CaO} + W_{MgO})/W_{Al_2O_3}$ to describe the basicity of slag and

Table III. Summary of Structure Viscosity Model, A, B, and C are Model Parameters, M_{oxide} is the Molar Fraction of Metal Oxide, W_{oxide} is the Weight Fraction of Metal Oxide

Sources	Structure Related Equation	Model Features	Error Deviation (Percent)
Urbain[51]	$\frac{W_{CaO}+W_{MgO}}{W_{Al_2O_3}}$	based on Frenkel-Weymann liquid viscosity model,[65] Urbain theoretically approved the linear correlation between A and B in Arrhenius-type equation	30.2
Riboud *et al.*[52]	$A = e^{(a\times(M_{CaO}+M_{MgO})-b\times M_{Al_2O_3}+c)}$ $B = a\times(M_{CaO}+M_{MgO})-b\times M_{Al_2O_3}+c$	based on Urbain model,[51] Riboud simplify the model equations and optimize the model parameters using viscosity data of blast furnace slag	61.0
Iida *et al.*[53]	$\frac{W_{CaO}\times a+W_{MgO}\times b}{W_{Al_2O_3}\times c+W_{SiO_2}\times d}$	Iida's model was developed based on slag basicity and own optimized parameters	68.6
Mill and Sridhar[54]	$\frac{M_{CaO}*a+M_{MgO}*b}{M_{Al_2O_3}*c+M_{SiO_2}*d}$	Mill's model was developed based on the oxides' optical basicity, which was reported by Duffy and Ingram[66]	70.4
Shankar[55]	$\frac{\frac{W_{CaO}\times a+W_{MgO}\times b}{W_{CaO}+W_{MgO}}}{\frac{M_{Al_2O_3}\times c+M_{SiO_2}\times d}{M_{Al_2O_3}+M_{SiO_2}}}$	Shankar optimized the model parameters and equation based on Mill's work[54]	55.2
Ray *et al.*[56]	$\frac{M_{CaO}\times a+M_{MgO}\times b}{M_{Al_2O_3}\times c+M_{SiO_2}\times d}$	Ray optimized the model parameters based on Mill's work[54]	51.5
Hu *et al.*[57]	$\frac{M_{CaO}-M_{Al_2O_3}+M_{MgO}\times b+2M_{SiO_2}\times c}{M_{MgO}+M_{CaO}-M_{Al_2O_3}+M_{Al_2O_3}\times c+2M_{SiO_2}}$	Hu also optimized the model parameters and equations based on Mill's work[54]	44.3
Gan and Lai[58]	$B = \sum b_{MO}M_{MO}$ $C = \sum c_{MO}M_{MO}$	Gan first proposed Vogel[67] -Fulcher[68] -Tammann[69] -type equation in SiO_2-Al_2O_3-CaO-MgO field, which can also predict the glass t transition temperature the blast furnace slag with slight modification	54.1
Tang *et al.*[59]	$\frac{\text{Non - brdging oxygen}}{SiO_4}$	Tang proposed the viscosity model using the ratio of nonbridging oxygen to silica content	63.9
Suzuki and Jak[60]	$E_a = E_{a,Si-Si}M_{Si-Si}+E_{a,Si-Me}M_{Si-Me}+E_{a,Me-Me}M_{Me-Me}$	Suzuki developed the viscosity model based on bond fraction, which was calculated by Factsage software. Suzuki's model contains large number of equations and parameters	35.1
FactSage[61,62]	Q^i-spices calculations to calculate E	FactSage model uses complicated expression to calculate the A and E in the Arrhenius-type equation	37.7
Shu[63]	$E = E_{SiO_2}M_{SiO_2}+E_{M_2SiO_4}M_{M_2SiO_4}+E_{Mo}M_{Mo}$	Shu developed the viscosity models based on compositions of three types of oxygen, which was calculated from optical basicity values	42.4
Zhang *et al.*[64]	$E_a = E_{a,bridging}M_{bridging}+E_{a,non-bridging}M_{non-bridging}+E_{a,free}M_{free}$	Zhang developed the viscosity models based on compositions of three types of oxygen, which was calculated from assumptions of connection correlation among $(AlO_4)^{5-}$, $(SiO_4)^{4-}$, Ca^{2+}, and Mg^{2+} in SiO_2-Al_2O_3-CaO-MgO system	28.5
Li *et al.*[20]	$a = \frac{\sum a_i\times x_i}{\sum x_i}$ $b = \frac{\sum b_i\times x_i}{\sum x_i}$	Li developed the model based on a new flow mechanism "cut-off" point	34.5

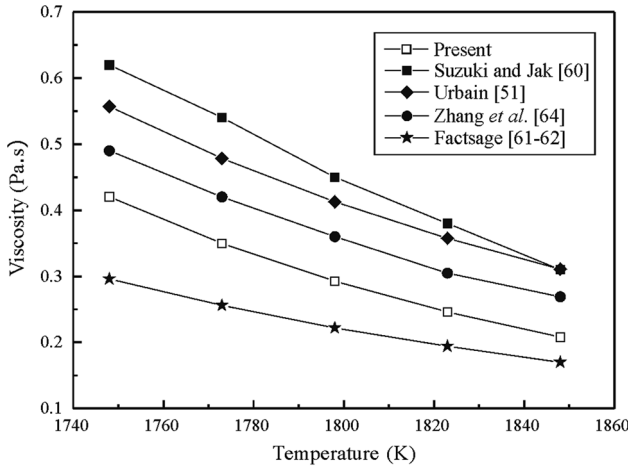

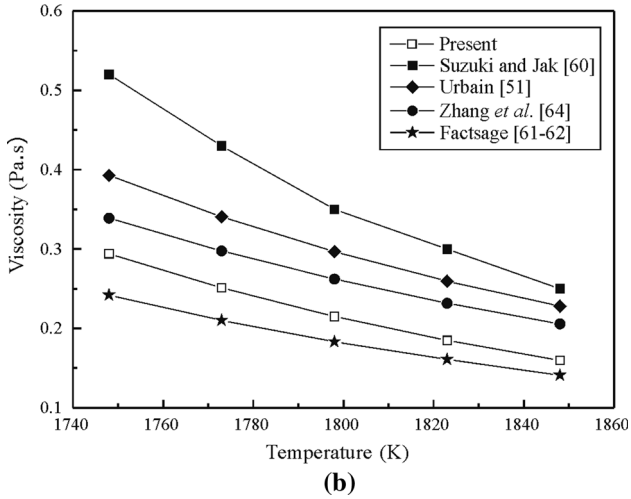

Fig. 5—Comparison of Urbain,[51] Suzuki and Jak,[60] FactSage[61,62] and Zhang *et al.*[64] model predictions and experimental data (*a*) 35.6 wt pct SiO_2, 15 wt pct Al_2O_3, 46.3 wt pct CaO, and 3 wt pct MgO (*b*) 33.1 wt pct SiO_2, 15 wt pct Al_2O_3, 42.9 wt pct CaO, and 9 wt pct MgO.

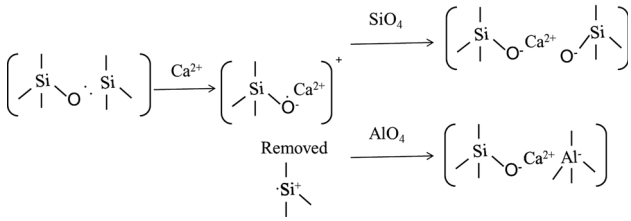

Fig. 6—Interaction among Ca^{2+} cations, $(SiO_4)^{4-}$, and $(AlO_4)^{5-}$.

predict viscosity. Riboud *et al.*[52] revised Urbain's work to predict the mold slag, which includes the CaO-SiO_2-Al_2O_3-MgO system. Mills and Sridhar[54] proposed viscosity models using optical basicity to describe the viscosity tendency with slag composition. Based on Mill's model, Shankar,[55] Ray *et al.*,[56] and Hu *et al.*[57] revised the model structures and parameters to improve the precision and accuracy on BF slags containing minor elements. Suzuki and Jak[60] decently investigated the impact of minor units within silicate structure to activation energy, which included over 100 equations and parameters for quaternary system. In addition, the core factor "bond fraction" of Suzuki's model[60] can only be calculated by FactSage Software. FactSage viscosity model[61,62] uses "Q-Species" from FactSage thermodynamic database to calculate the viscosity. Shu[63] and Zhang *et al.*[64] established viscosity models with consideration of three type's oxygen O, O^-, and O^{2-}. However, the calculation of oxygen concentration is lack of theory support and relies on assumption.[63,64] The features of the existing viscosity models are summarized in Table III.

B. *Model Performance Evaluation*

14 structural models were reviewed and evaluated in the present study using the accepted viscosity database. Equation [6] is used to calculate difference between the measured and the calculated viscosity values. The evaluation results have been summarized in Table III.

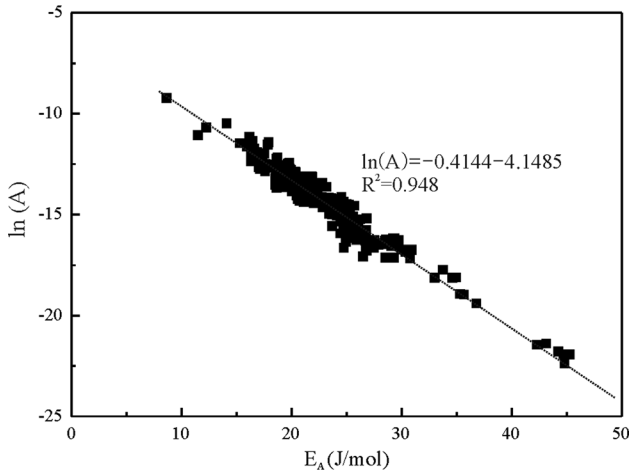

Fig. 7—The linear relationship between E_A and ln(A).

Table IV. Viscosities Measured by the Present Authors

Experiment Number	Compositions (Weight Percent)				Viscosities (Pa s)				
	SiO_2	Al_2O_3	CaO	MgO	1748 K (1475 °C)	1773 K (1500 °C)	1798 K (1525 °C)	1823 K (1550 °C)	1848 K (1575 °C)
1	35.6	15	46.4	3	0.41	0.34	0.29	0.25	0.21
2	33	15	42.9	9	0.3	0.25	0.21	0.19	0.16

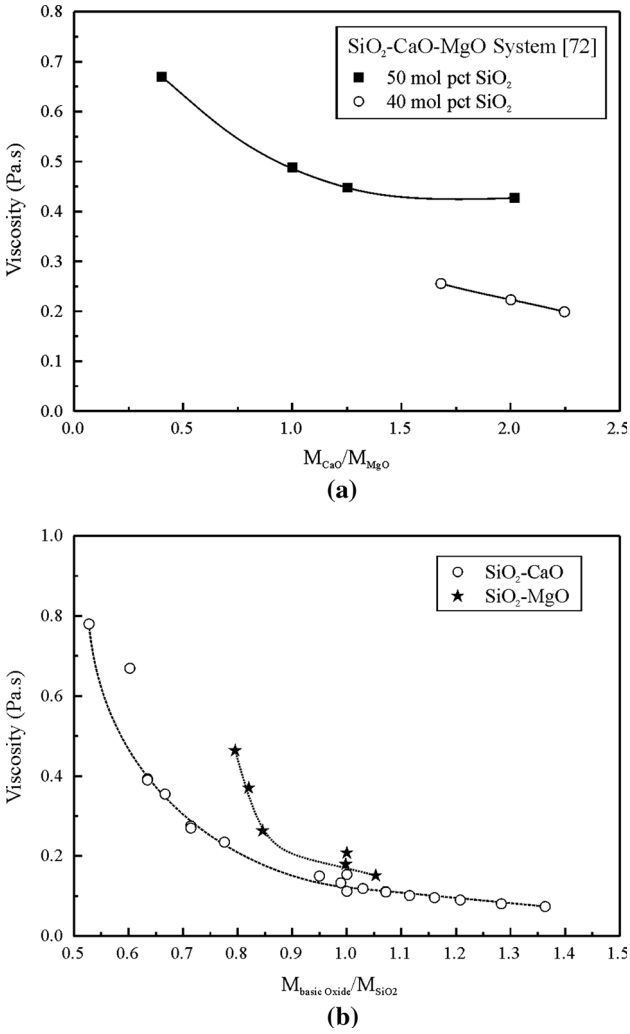

Fig. 8—(*a*) Viscosity measurements in SiO_2-CaO-MgO system with 40 and 50 mol pct SiO_2 at 1773 K (1500 °C) from Licko and Danek[72]; (*b*) SiO_2-CaO and SiO_2-MgO system at 2123 K (1850 °C) from Bockris *et al.*[46]

$$\Delta = \frac{1}{n} \times \sum \frac{|\eta_{\text{exp}} - \eta_{\text{Calc}}|}{\eta_{\text{exp}}}, \qquad [6]$$

where Δ is the average deviation, η_{exp} is the experimental viscosity, η_{Calc} is the calculated viscosity, and n is the number of data.

It can be seen that the relative error ranges are between 28 and 70 pct in full composition range. The models of Urbain[51] and Zhang *et al.*[64] reported the lowest relative errors 30.2 and 28.5 pct, respectively.

Four viscosity models with relative good performances are selected for further comparison with the experimental data. As shown in Table IV, viscosities of two synthetic BF slags were measured by the present authors to evaluate the viscosity models.[6] It can be seen from Figures 5(a) and (b) that, in general, the four models can reasonably reproduce the measurements. FactSage[61,62] tends to underestimate the viscosities and other three models[51,60,64] overestimate the viscosities. Zhang *et al.*'s model[64] has the best performance reporting 15 pct deviations to the experimental data of these compositions.

IV. CONSTRUCTION OF NEW VISCOSITY MODEL

A. *Silicate Structure*

The viscosity of molten slag closely related to its structure, which is dependent on composition and temperature. It is widely accepted that basic oxides tend to break Si-O-Si bond in silicate network and forms $Si\text{-}O^-$ intermediate (also known as nonbridging oxygen). Also, amphoteric oxide Al_2O_3 can form $(AlO_4)^{5-}$ unit to connect with $(SiO_4)^{4-}$ network, which require cations (Ca^{2+} or Mg^{2+}) charge compensation. As shown in Figure 6, the major role of Ca^{2+}/Mg^{2+} is to break the $(SiO_4)^{4-}$ network and compensate the $(AlO_4)^{5-}$ charges. This intermediate Ca(Mg)-SiO_4 structure unit has one free positive charge, which is able to break another SiO_4 or compensate the AlO_4 charges.

Al_2O_3 can behave as either acidic oxide or basic oxide depending on the concentrations of basic oxides. If sufficient Ca^{2+} and Mg^{2+} cations are present to balance the $(AlO_4)^{5-}$ charges, Al_2O_3 acts as an acidic oxide which is incorporated into the silicate network in tetrahedron coordination. In the case of insufficient basic oxides, Al^{3+} will behave the same as Ca^{2+} or Mg^{2+} to break the (SiO_4) network.[70]

In the present SiO_2-Al_2O_3-CaO-MgO system, due to electrical force between charges, it is presumed that when Ca^{2+}/Mg^{2+} concentration is low, they have higher priority to balance the $(AlO_4)^{5-}$ charges than breaking the Si-O covalent bonds.[50]

B. *Temperature Dependence*

The temperature dependence of viscosity can be described by the Arrhenius-type equation (Eq. [7]).[49]

$$\eta = A \times \exp\left(\frac{1000 \times E_A}{T}\right), \qquad [7]$$

where η is the viscosity in Pa s, T is the absolute temperature in K, A is the pre-exponential factor, E_A represents the integral activation energy in J/mol.

C. *Pre-exponential Factor A*

As shown in Eq. [8], a linear relationship between pre-exponent factor A and activation energy E_A was proposed by Urbain.[51] The activation energy E_A and pre-exponential factor A can be determined by plotting $\ln(\eta)$ against $1/T$ under the same composition.

$$\ln A = -m \times E_A - n. \qquad [8]$$

This linear correlation has been widely applied in different viscosity models, such as the Shankar's[55] and Hu *et al.*'s models.[57] In the present study, from accepted viscosity data, the linear correlation is confirmed as shown in Figure 7. $\ln(A)$ and E_A have a linear

relationship with $R^2 = 0.948$, which will be used in construction of the present viscosity model. m and n values in Eq. [8] are 0.4144 and 4.1485, respectively.

D. *Network Modifier Probability*

With the study of silicate-based mineralogy, Ramberg[71] suggests that the silicate structure (polymerized level of SiO_4 network) is dependent on basic oxide concentrations, atomic radius, and electronegativity. Review of the viscosity measurements in SiO_2-CaO-MgO ternary system by Licko and Danek[72] shows that the replacement of CaO by MgO will reduce the slag viscosity. As shown in Figure 8(a), at 1773 K (1500 °C), the increasing M_{CaO}/M_{MgO} ratio cause viscosity reduction at both 40 and 50 mol pct SiO_2 conditions. The viscosity measurements by Bockris *et al.*[46] in SiO_2-CaO and SiO_2-MgO binary systems support this conclusion as shown in Figure 8(b). At 2123 K (1850 °C), at the same basic oxide concentration, the viscosity of SiO_2-CaO system is larger than SiO_2-MgO system. Through continuously basic oxide additions, the viscosity differences between SiO_2-CaO and SiO_2-MgO system decreases. In the existing viscosity models of SiO_2-Al_2O_3-CaO-MgO system, few researchers discussed the distribution of cations (Ca^{2+} or Mg^{2+}) in SiO_4 and AlO_4 network structure except for Zhang's model.[64]

In the present study, "probability (P)" is introduced to describe the fraction of cations (Ca^{2+} or Mg^{2+}) to break the Si-O network and the rest ($1 - P$) will be used for charge compensation of $(AlO_4)^{5-}$ tetrahedral units. It is related to the electronegativity of Ca^{2+}, Mg^{2+}, $(SiO_4)^{4-}$, and $(AlO_4)^{5-}$ and their molar fractions. At low concentration of CaO/MgO, there is a high probability to compensate the $(AlO_4)^{5-}$ charges. When the concentration of CaO/MgO increases, the probability of breaking Si-O will raise.

$$P_{Ca} = \frac{\chi_{Ca^{2+}} M_{Ca^{2+}}}{\chi_{(SiO_4)^{4-}} \times M_{(SiO_4)^{4-}} + \chi_{(AlO_4)^{5-}} \times M_{(AlO_4)^{5-}}} \quad [9]$$

$$P_{Mg} = \frac{\chi_{Mg^{2+}} M_{Mg^{2+}}}{\chi_{(SiO_4)^{4-}} \times M_{(SiO_4)^{4-}} + \chi_{(AlO_4)^{5-}} \times M_{(AlO_4)^{5-}}}, \quad [10]$$

Table V. Electronegativity χ of Basic Oxide Cations and Network Former Units

	Ca^{2+}	Mg^{2+}	(AlO_4)	(SiO_4)
X	3.07	3.82	6.674	6.985

where M is molar fraction of metal oxide; χ is electronegativity of structure units in slag system.

The electronegativity χ of Ca^{2+}, Mg^{2+}, AlO_4, and SiO_4 units are determined using Revised–Mulliken Electronegativity,[73] which is derived from first ionization energy and electron affinity of the atom. The values of electronegativity are shown in Table V.

$$\chi = \frac{I + E}{2}, \quad [11]$$

where I is the ionization energy (kJ/mol) and E is electron affinity (kJ/mol).

E. *Activation Energy E_A*

In the present study, E_A is defined as the integral activation energy of silicate slag, which is composed of four metal oxides and can be expressed as

$$E_A = E_{CaO} + E_{MgO} + E_{Al_2O_3} + E_{SiO_2}, \quad [12]$$

where E_i is activation energy of i component (i = SiO_2, Al_2O_3, CaO and MgO), which is calculated using Eqs. [13] through [16].

$$E_{CaO} = E^0_{Ca} + E_{SiO_4-Ca-SiO_4} \times P^2_{Ca} + E_{SiO_4-Ca-AlO_4} \times P_{Ca} \times (1 - P_{Ca}) \quad [13]$$

$$E_{MgO} = E^0_{Mg} + E_{SiO_4-Mg-SiO_4} \times P^2_{Mg} + E_{SiO_4-Mg-AlO_4} \times P_{Mg} \times (1 - P_{Mg}) \quad [14]$$

$$E_{Al} = E^0_{Al} + E_{Al-3SiO_4} \times \left[1 - (1 - P_{Ca}) \times (1 - P_{Mg})\right]^3 + E_{AlO_4-Ca-AlO_4} \times (1 - P_{Ca})^2 + E_{AlO_4-Mg-AlO_4} \times (1 - P_{Mg})^2 \quad [15]$$

$$E_{SiO_2} = E_{SiO_4}. \quad [16]$$

In SiO_2-Al_2O_3-CaO-MgO system, as a network modifier, three structure units are relevant to CaO including free oxygen O^{2-}, SiO_4-Ca-SiO_4, and SiO_4-Ca-AlO_4. As defined before, P_{Ca} represents the probability of one Ca^{2+} cation connecting with one SiO_4 tetrahedron, and $(1 - P_{Ca})$ is the probability to compensate the $(AlO_4)^-$ charges. Therefore, the probabilities of SiO_4-Ca-SiO_4 and SiO_4-Ca-AlO_4 can be calculated by P^2_{Ca} and $P_{Ca} \times (1 - P_{ca})$, respectively. As Eq. [13] shows, the

Table VI. Activation Energy Parameters of All Involved Structural Units in SiO_2-Al_2O_3-CaO-MgO System

Basic Oxide				Acidic Oxide			
Ca-O	−0.314	Mg-O	−0.24	Si	7.21	Al-O	−0.24
Si-Ca-Si	−7.386	Si-Mg-Si	−9.092			3Al-Si	−0.53
Si-Ca-Al	−0.711	Si-Mg-Al	−0.511			Al-Ca-Al	23.78
						Al-Mg-Al	15.83

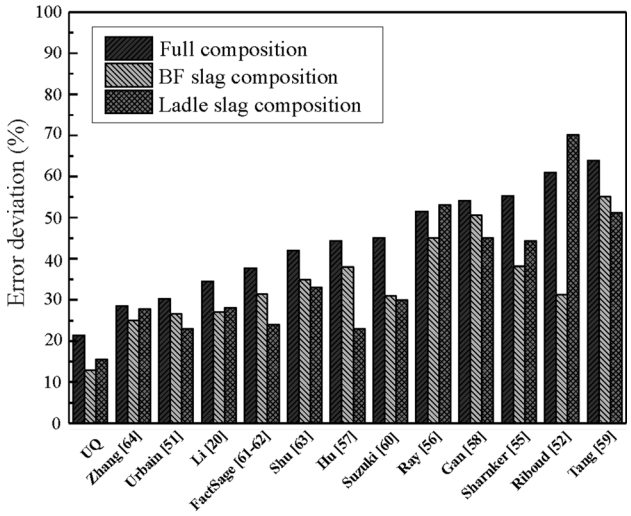

Fig. 9—The performance summary of viscosity models in three different composition ranges.

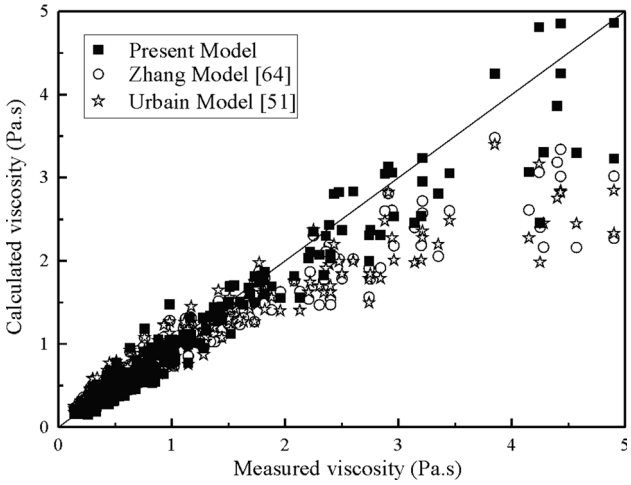

Fig. 10—Comparison of experimental viscosity and calculated viscosity between present model, Zhang's model[64] and Urbain's model.[51]

integral activation energy of CaO is calculated by sum of energy contributions of each structural unit multiplied by its probability. The E_{Ca}^{0} is the constant representing O^{2-} from CaO. Similarly, the calculation of MgO integral energy is expressed in Eq. [14].

As an amphoteric oxide, Al_2O_3 shows both negative and positive impacts on activation energy. There are four possible structure units for aluminum cations: network modifier unit (O^{2-}), 3(SiO_4)-Al, and network former unit (AlO_4-Ca-AlO_4 and AlO_4-Mg-AlO_4). The charge balanced AlO_4-Ca/Mg structure units give a positive contribution to the integral activation energy. The $(1 - P_{Ca})$ and $(1 - P_{Ca})$ are used to describe the probability of Ca^{2+}/Mg^{2+} participating on alumina network. One Ca^{2+}/Mg^{2+} cation is able to balance two $(AlO_4)^{5-}$ structure units, and therefore, the probabilities of AlO_4-Ca-AlO_4 and AlO_4-Mg-AlO_4 are calculated by $(1 - P_{Ca})^2$ and $(1 - P_{Mg})^2$. 3(SiO_4)-Al represents the network breaking effect of Al^{3+} cation and shows a negative contribution to activation energy. The Al^{3+}, which is not charge compensated, can be described as $(1 - (1 - P_{Ca}) \times (1 - P_{Mg}))$. One Al^{3+} can compensate three $(SiO_4)^{4-}$ units. Therefore, the probability of Al^{3+} connecting with 3 $(SiO_4)^{4-}$ can be written as $(1 - (1 - P_{Ca}) \times (1 - P_{Mg}))^3$. The E_{Ar}^{0} is a constant activation energy representing free O^{2-} from Al_2O_3. However, due to charge compensation, most of O^{2-} contributes into $(AlO_4)^{5-}$ network, which reflects small activation energy in Table VI. Therefore, the calculation of Al_2O_3 integral energy is expressed in Eq. [15].

Silica is assumed to be fully polymerized and only exists one structure unit $(SiO_4)^{4-}$. It is considered to be the base structure unit of silicate and the parameter for E_{SiO_4} is a constant as shown in Table VI. The calculation of SiO_2 integral energy is expressed in Eq. [16].

The overall activation energy of all structure units is optimized from collected viscosity data in the SiO_2-Al_2O_3-CaO-MgO system. From the parameters in Table VI, the major structural unit in network breaking is Si-Ca(Mg)-Si. The free O^{2-} and Si-Ca(Mg)-Al have less significant impacts on the activation energy. In addition, CaO has higher priority to compensate the AlO_4 charges and lower priority for SiO_4 charges, which is demonstrated by the optimized parameters.

F. *Performances of the New Model*

The performance of the current model is evaluated by comparison with other models using the viscosity data in the SiO_2-Al_2O_3-CaO-MgO system. The mean deviation Δ is calculated using Eq. [6].

1. *SiO_2-Al_2O_3-CaO-MgO system*

The evaluations of the model performances were carried out with respect to the following data: (i) all viscosity data in the SiO_2-Al_2O_3-CaO-MgO system; (ii) slag composition in the blast furnace : 30 to 40 wt pct SiO_2, 10 to 20 wt pct Al_2O_3, 30 to 45 wt pct CaO, and 5 to 10 wt pct MgO; and (iii) slag composition in the ladle: 10 to 25 wt pct SiO_2, 20 to 30 wt pct Al_2O_3, 40 to 50 wt Pct CaO, and 5 to 10 wt pct MgO.

The results for model comparison are shown in Figure 9. It can be seen that the present model performs very well in all composition ranges, with the mean deviation 21.4 pct in the full composition, 12.5 pct in the BF slag composition, and 15.5 pct in the ladle slag composition range.

A detailed comparison is conducted using three most accurate models: present model, Zhang's model,[64] and Urbain's model[51] at the viscosity range of 0 to 5 Pa s. It can be seen from Figure 10, the present model has overall superior performance than both Zhang's[64] and Urbain's[51] models. The mean deviation is 12.5, 19.4, and 19.3 pct for the present model, Zhang's model, and Urbain's model, respectively. At high value ranges (>2 Pa s), the present model prediction distributed on both sides of the experiment viscosity. In contrast, the

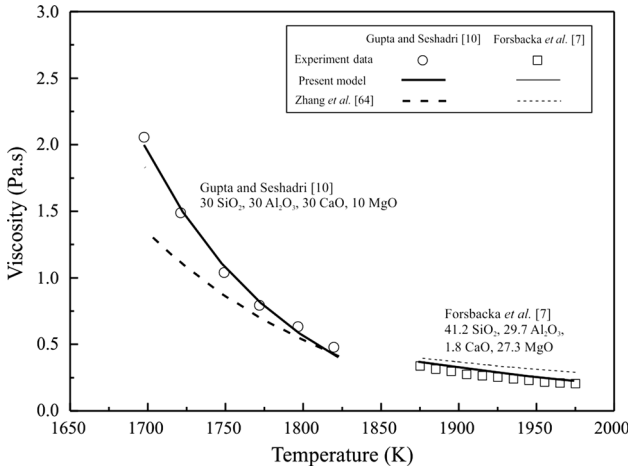

Fig. 11—Comparisons between model predictions and experimental results from Gultyai[9] and Hofmann[12] at 1773 K (1500 °C) in the SiO_2-Al_2O_3-CaO-MgO system.

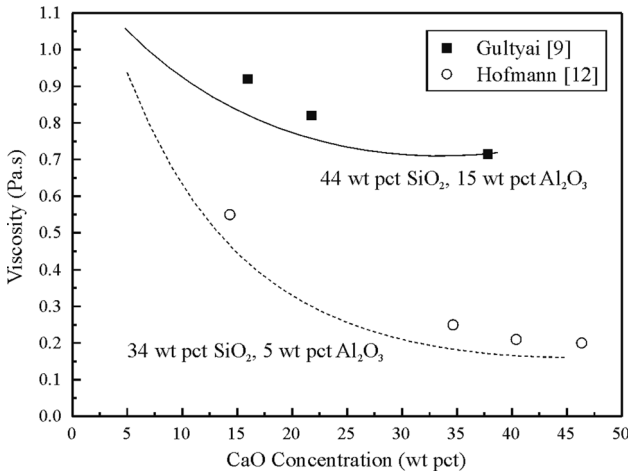

Fig. 12—The linear relationship between E_A and ln(A) for SiO_2-Al_2O_3-CaO and SiO_2-Al_2O_3-MgO systems.

Urbain's and Zhang's models tend to underestimate the experimental data. Furthermore, the temperature dependence of present model was evaluated and compared with Zhang's model.[64] As shown in Figure 11, at two different temperature ranges [1698 K to 1823 K (1425 °C to 1600 °C) and 1923 K to 1993 K (1650 °C to 1720 °C)], the present model shows a good agreement with the experimental data.[7,10] Zhang's model[64] well reproduces the experimental data at high temperature ranges with viscosity values lower than 1 Pa s, but shows lower predictions comparing with the data from Gupta and Seshardri.[10]

2. *Predictions of viscosity trend*

The impacts of CaO and MgO on viscosity are investigated using model prediction and experimental data. At fixed SiO_2, Al_2O_3 and temperature [1773 K (1500 °C)], as shown in Figure 12, the replacement of MgO by CaO content was evaluated under two compositions: (1) high acidic oxide (44 wt pct SiO_2, 15 wt pct Al_2O_3) and (2) low acidic oxide (33 wt pct SiO_2 and 5 wt pct Al_2O_3). In both conditions, through CaO replacement, the slag viscosities decrease and decrement slope continuously reduced. Because of charge compensation impact of SiO_4 and AlO_4 units, the viscosity decrement is more sensitive at low acidic oxide concentrations. The model predictions agree well with experimental data by Gultyai[9] and Hofmann.[12]

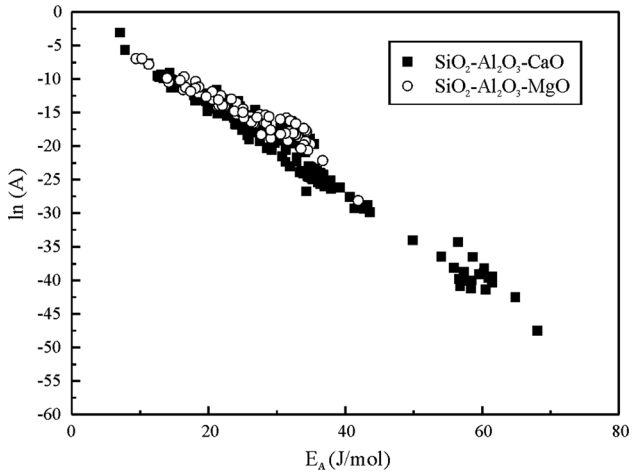

Fig. 13—The linear relationship between E_A and ln(A) for SiO_2-Al_2O_3-CaO from Hofmann,[12] Bills,[74] Johannsen and Brunion,[14] Machin *et al.*,[35–37] Urbain *et al.*,[75] Yasukouchi *et al.*,[77] Tunezo and Kawai,[78] Zhang and Chou,[79] Toplis and Dingwell[80] and SiO_2-Al_2O_3-MgO systems from Johannsen and Brunion,[14] Lyutikov and Tsylev,[76] Toplis and Dingwell.[80]

3. *Subternary and subbinary systems*

The present model can also be used to predict the low-order silicate systems containing CaO, MgO, and Al_2O_3. As shown in Figure 13, the linear relationship between activation energy E_A and pre-exponential factor B can also be applied for lower-order systems with different m and n values in Eq. [8]. For each binary or ternary system, the individual m and n values were used to minimize the prediction deviation. The values of m, n, and prediction deviation for each system are summarized in Table VII.

The experimental viscosity data for the systems of SiO_2-Al_2O_3-CaO, SiO_2-Al_2O_3-MgO, SiO_2-CaO, SiO_2-MgO, and SiO_2-Al_2O_3 are evaluated with calculated values by the present model. The error deviations of different systems are shown in Table VII which shows the predicted viscosities by the present model reasonably agree with reported data. Higher error deviations are reported in two ternary systems indicating that current model needs to be improved to better describe amphoteric behavior of Al_2O_3 in extreme conditions (very high Al_2O_3 concentration). Note that all available viscosity data in the ternary and binary systems have been used.

Table VII. The Summary of Model Parameters in Binary and Ternary Silicate System Containing CaO, MgO, and Al_2O_3

	m	n	Error Deviation (Percent)	Database
SiO_2-Al_2O_3-CaO	0.5953	2.668	28.9	Hofmann,[12] Bills,[74] Johannsen and Brunion,[14] Machin *et al.*,[35–37] Urbain *et al.*[75] Yasukouchi *et al.*[77] Tunezo and Kawai[78] Zhang and Chou[79] Toplis and Dingwell[80]
SiO_2-Al_2O_3-MgO	0.3831	1.442	28.6	Johannsen and Brunion,[14] Lyutikov and Tsylev[76] Toplis and Dingwell[80]
SiO_2-CaO	0.5741	2.311	20.1	Bockris *et al.*,[46] Urbain *et al.*[75] Yasukouchi *et al.*[77] Tunezo and Kawai[78]
SiO_2-MgO	0.4468	1.532	15.4	Bockris *et al.*,[46] Hofmann,[12] Urbain *et al.*[75]
SiO_2-Al_2O_3	0.5359	2.371	12.9	Bockris *et al.*,[46] Urbain *et al.*[75] Yasukouchi *et al.*[77]

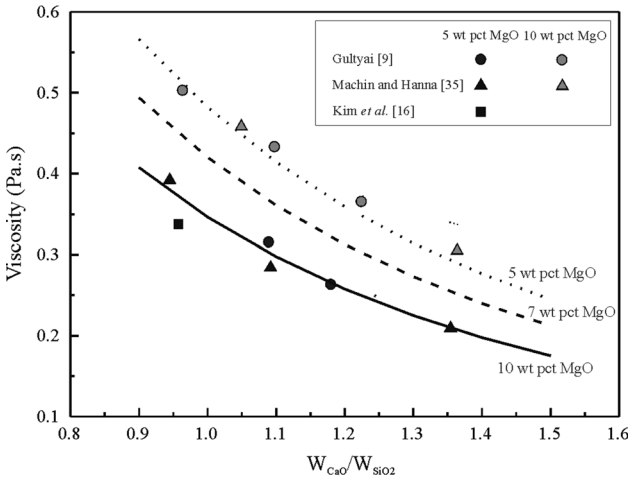

Fig. 14—Effects of W_{CaO}/W_{SiO_2} and MgO on slag viscosities at 1773 K (1500 °C) with fixed 15 wt pct Al_2O_3 calculated by present model in comparisons with the data from Kim *et al.*,[16] Gultyai,[9] and Machin and Hanna.[35]

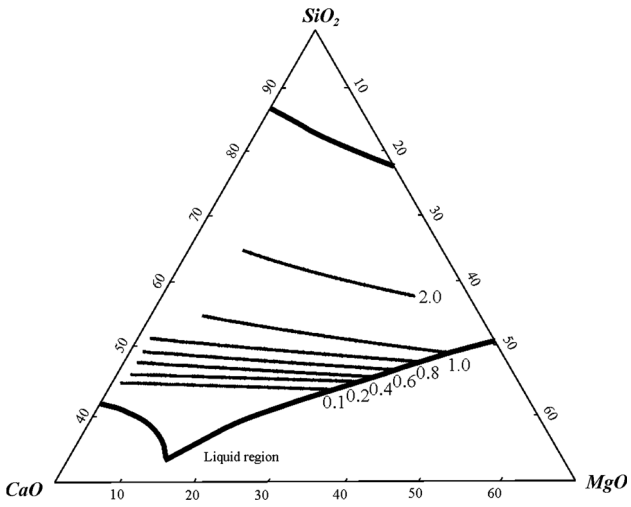

Fig. 15—The model prediction of isoviscosity diagram at 1773 K (1500 °C) with fixed 15 wt pct Al_2O_3.

V. INDUSTRIAL IMPLICATIONS

A. *Blast Furnace Slags for Ironmaking process*

Examples of the industrial applications using the developed viscosity model are demonstrated in this section. Figure 8 shows effect of (W_{CaO}/W_{SiO_2}) on viscosity of blast furnace slag at 15 wt pct Al_2O_3 and various MgO concentrations at 1773 K (1500°C). It can be seen that predictions agree well with the data of Kim *et al.*,[16] Gultyai,[9] and Machin and Hanna[35]. At a given Al_2O_3 and MgO concentration, the addition of CaO continuously decreases the slag viscosity. Also, it indicates that at a given W_{CaO}/W_{SiO_2}, the slag viscosities decrease with increasing MgO concentration. The effect of MgO seems to be more significant at low W_{CaO}/W_{SiO_2}. MgO is usually added in the BF operation as flux. Reduction of MgO can decrease the direct cost in material and also fuel consumptions. It can be seen from Figure 14 that reduced MgO will increase the slag viscosity. To keep the slag viscosity at a low-level, W_{CaO}/W_{SiO_2} needs to be increased. However, liquidus temperature has to be controlled to avoid formation of solid phase at operating temperature.

The present viscosity model can only predict viscosities for single liquid phase. It is essential to make sure the slag is liquid before the viscosity is calculated by the viscosity model. It is therefore necessary to present isoviscosity lines on the phase diagram. As an example, the isoviscosity lines are calculated using the present viscosity model for blast furnace slags at 1773 K (1500 °C) and 15 wt pct Al_2O_3. In Figure 15, all viscosities are presented within the fully liquid region. It can be seen from the figure that clearly, the viscosity is mainly dependent of SiO_2 concentration. The isoviscosity lines are almost parallel to the CaO-MgO axis, which has bias down to the MgO direction. It is indicated that the replacement of CaO by MgO will slightly decrease the slag viscosity at fixed SiO_2 concentration. This behavior is consistent with the fact that the viscosity parameters of E_{Mg} is higher than E_{Ca} as network modifier, which also matches the conclusion from review

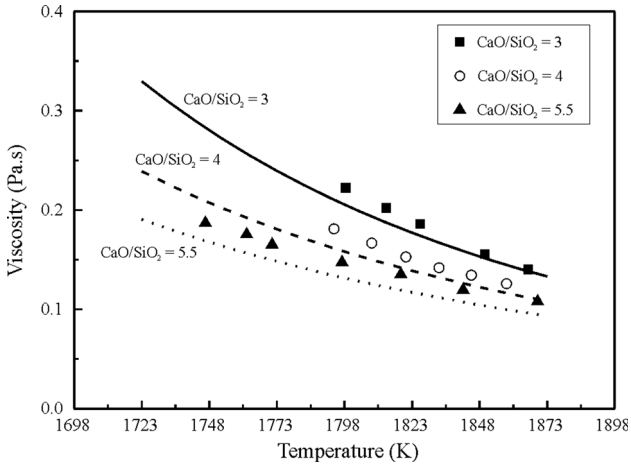

Fig. 16—Effects of W_{CaO}/W_{SiO_2} and temperature on slag viscosities with fixed 5 wt pct MgO and 30 wt pct Al_2O_3 by present model in comparisons with data from Song *et al.*[30]

of binary viscosity data of SiO_2-CaO and SiO_2-MgO systems.

B. *Ladle Slags for Steelmaking Process*

In steelmaking process, the desired viscosity of ladle slag (0.2 to 0.4 Pa s) is lower than BF final slag (0.4 to 0.6 Pa s).[74] Figure 16 shows effects of temperature and slag basicity on viscosity at 30 wt pct Al_2O_3 and 5 wt pct MgO. The present model can well predict Song *et al.*'s data[30] with average deviation 15 pct. At fixed Al_2O_3 and MgO concentrations, the viscosities decrease significantly with increasing W_{CaO}/W_{SiO_2} ratio and the decrement is more significant at low temperatures. For example, the viscosity is decreased by approximately 0.13 Pa s at 1723 K (1450 °C) when W_{CaO}/W_{SiO_2} is increased from 3 to 5.5. At 1823 K (1550 °C), the decrement of the viscosity is only approximately 0.05 Pa s when W_{CaO}/W_{SiO_2} is increased from 3 to 5.5.

VI. CONCLUSIONS

Viscosity data and models in the system SiO_2-Al_2O_3-CaO-MgO have been critically reviewed and evaluated. 3135 viscosity data for 607 compositions have been collected from 37 papers and carefully examined based on (1) experimental techniques, (2) data consistency, and (3) cross-reference comparisons. 1780 viscosity measurements from 10 to 65 wt pct SiO_2, 3.5 to 40 wt pct Al_2O_3, 2 to 60 wt pct CaO, and 2 to 38 wt pct MgO composition have been accepted to the database for viscosity model evaluation and development. 14 structure-based viscosity models have been critically reviewed for their structures, parameters, applicable slag systems, and prediction performance. By comparing with the accepted viscosity data, it has been found that the relative error ranges between 28.5 and 70 pct in full composition range. All information will be utilized for further development of the viscosity model to improve the prediction performance.

An accurate viscosity model has been developed in the system SiO_2-Al_2O_3-CaO-MgO using a large number of critically reviewed experimental data. A new term 'probability' based on composition and electronegativity was introduced to describe the distribution of cations within the acidic oxide. The new model can accurately predict viscosities for blast furnace slags and steel refining slags in the system SiO_2-Al_2O_3-CaO-MgO. The model developed also has good performance for the subsystems SiO_2-Al_2O_3-CaO, SiO_2-Al_2O_3-MgO, SiO_2-Al_2O_3, SiO_2-CaO, and SiO_2-MgO.

ACKNOWLEDGMENTS

The authors would like to acknowledge the financial support from Shougang Group, China and Rio Tinto Iron Ore, Australia.

REFERENCES

1. A.K. Biswas: *Principles of Blast Furnace Ironmaking*, 2nd ed., Cootha Publication House, Brisbane, 1981, p. 329.
2. C. Wu, Y.Q. Sum, D.X. Luo, and Y.X. Lu: *J. Wuhan Univ. Sci. Technol.*, 2013, vol. 36, pp. 254–57.
3. J.W. Matousek: *Min. Met. Mater. Soc.*, 2015, vol. 67, pp. 1216–22.
4. L. Zhou, X.H. Wang, and J. Wang: *J. Iron Steel Res.*, 2014, vol. 21, pp. 70–3.
5. K.C. Mills and S. Sridhar: *Ironmak. Steelmak.*, 1999, vol. 26, pp. 262–68.
6. M Chen, D Zhang, M Kou, and B Zhao: *ISIJ Int.*, 2014, vol. 54, pp. 2025–30.
7. L. Forsbacka, L. Holappa, T. Iida, Y. Kita, and Y. Toda: *Scand. J. Metall.*, 2003, vol. 32, pp. 273–80.
8. Y.M. Gao, S.B. Wang, C. Hong, X.J. Ma, and F. Yang: *Int. J. Min. Metall. Mater.*, 2014, vol. 21, pp. 353–62.
9. I. Gul'tyai: *Izv. Akad. Nauk SSSR*, 1962, vol. 5, pp. 52–65.
10. V.K. Gupta and V. Seshadri: *Trans. Indian Inst. Met.*, 1973, vol. 26, pp. 55–64.
11. J.W. Han, E.H. Kwon, S.S. Han, J.H. Chi, B.S. Kim, and J.C. Lee: *Mater. Sci. Forum*, 2003, vol. 439, pp. 149–55.
12. E.E. Hofmann: *Berg- und hüttenmännische monatshefte*, 1959, vol. 106, pp. 397–407.
13. E.E. Hofmann: *Stahl Eisen*, 1959, vol. 79, pp. 846–53.
14. F. Johannsen and H. Brunion: *Zeitschrift fur Erzbergbau und Metallhutten-Wesen*, 1959, vol. 12, pp. 272–79.
15. Y. Kawai: *The science reports of the Research Institutes*, Tohoku University, Physics, 1952, vol. A, pp. 615–21.
16. H. Kim, H. Matsuura, F. Tsukihashi, W. Wang, D.J. Min, and I. Sohn: *Metall. Mater. Trans. B*, 2012, vol. 44B, pp. 5–12.
17. J.R. Kim, Y.S. Lee, and D.J. Min: *ISSTech. Conference*, 2003, Indianapolis, USA, p. 515.
18. S.H. Kim and J.D. Seo: *Iron Steelmak.*, 1999, vol. 26, pp. 51–7.
19. T. Koshida, T. Ogasawara, and H. Kishidaka: *Tetsu to Hagane*, 1981, vol. 67, pp. 1491–97.
20. P.C. Li and X.J. Ning: *Metall. Mater. Trans. B*, 2016, vol. 47B, pp. 446–57.
21. Y.S. Lee, J.H. Park, D.J. Min, S.H. Yi, and W.W. Huh: *Ironmaking Conf. Proc.*, 2002, vol. 61, pp. 155–65.
22. Y.S. Lee, D.J. Min, S.M. Jung, and S.H. Yi: *ISIJ Int.*, 2004, vol. 44, pp. 1283–89.
23. U. Mishra, B. Thakur, and M. Thakur: *SEAISI Q.*, 1994, vol. 23, pp. 72–82.
24. A.M. Muratov and I.S. Kulikov: *Izvestiya Akademii Nauk SSSR Metally*, 1965, vol. 1, pp. 57–62.
25. M. Nakamoto, T. Tanaka, J. Lee, and T. Usui: *ISIJ Int.*, 2004, vol. 44, pp. 2115–19.

26. H. Park, J.Y. Park, G.H. Kim, and I. Sohn: *Steel Res. Int*., 2012, vol. 83, pp. 150–56.
27. N. Saito, N. Hori, K. Nakashima, and K. Mori: *Metall. Mater. Trans. B*, 2003, vol. 34B, pp. 509–11.
28. C. Scarfe, D. Cronin, J. Wenzel, and D. Kauffman: *Am. Mineral*., 1983, vol. 68, pp. 1083–88.
29. A. Shankar, M. Görnerup, A.K. Lahiri, and S. Seetharaman: *Metall. Mater. Trans. B*, 2007, vol. 38B, pp. 911–15.
30. M. Song, Q. Shu, and D. Sichen: *Steel Res. Int*., 2011, vol. 82, pp. 260–68.
31. XL Tang, ZT Zhang, M Guo, M Zhang, and XD Wang: *J. Iron Steel Res. Int*., 2011, vol. 18, pp. 1–17.
32. G.P. Vyatkin, N.L. Zhilo, and M.Y. Ostroukhov: Izvestiya Vysshikh Uchebnykh Zavedenii. Chernaya*Metallurgia*., 1962, vol. 5, pp. 25–9.
33. L. Yao, S. Ren, X.Q. Wang, Q.C. Liu, L.Y. Dong, J.F. Yang, and J.B. Liu: *Steel Res. Int*., 2016, vol. 87, pp. 241–49.
34. Y. Kita, A. Handa, and T. Iida: *J. High Temp. Soc. Japan*, 2001, vol. 27, pp. 144–50.
35. J.S. Machin and D.L. Hanna: *J. Am. Ceram. Soc*., 1945, vol. 28, pp. 310–16.
36. J.S. Machin and T.B. Yee: *J. Am. Ceram. Soc*., 1954, vol. 37, pp. 177–86.
37. J.S. Machin, T.B. Yee, and D.L. Hanna: *J. Am. Ceram. Soc*., 1952, vol. 35, pp. 322–25.
38. L.N. Sheludyakov, E.T. Sarancha, and A.A. Vakhitov: *Trans. Inst. Khim. Nauk, Akad. Nauk Kaz. SSR*, 1967, vol. 15, pp. 158–63.
39. A.I. Tsybulnikov, G.A. Toporishchev, G.A. Vachugov, E.D. Mokhir, and V.V. Vetysheva: *Izvestiya Vysshikh Uchebnykh Zavedenii. Chernaya Metallurgia*, 1973, vol. 2, pp. 5–9.
40. A.M. Yakushev, V.M. Romashin, and V.A Amfiteatrov: *Izvestiya Vysshikh Uchebnykh Zavedenii. Chernaya Metallurgia*, 1977, vol. 55–58.
41. M. Kato and S. Minowa: *Trans. Iron Steel Inst. Jpn*., 1969, vol. 9, pp. 31–38.
42. H. Taniguchi: *Contrib. Mineral. Petrol*., 1992, vol. 109, pp. 295–303.
43. VDEh: *Slag Atlas*, 2nd edn, Verlag Stahleisen, Dusseldorf, 1995, p. 351.
44. G Leblanc, R Secco, and M Kostic: *The Measurement, Instrumentation and Sensors Handbook*, Springer, Berlin, 1999, p. 1.
45. E.F. Riebling: *Rev. Sci. Instrum*., 1963, vol. 34, pp. 568–72.
46. J.O.M. Bockris, J.D. Mackenzie, and J.A. Kitchener: *Trans. Faraday Soc*., 1955, vol. 51, pp. 1734–48.
47. C. Bale, P. Chartrand, S. Degterov, G. Eriksson, K. Hack, R. Ben Mahfoud, J. Melançon, A. Pelton, and S. Petersen: *Calphad*, 2002, vol. 26, pp. 189–228.
48. M. Chen, D.W. Zhang, and B. Zhao: *Proceeding of 4th Australia-China-Japan Joint Symposium on Iron and Steel-making*, Shenyang, China, 2012, pp. 115–27.
49. S. Sathivel, J. Huang, and W. Prinyawiwatkul: *J. Food Eng*., 2008, vol. 84, pp. 187–93.
50. I. Sohn and D.J. Min: *Steel Res. Int*., 2012, vol. 83, pp. 611–30.
51. G. Urbain: *Steel Res. Int*., 1987, vol. 58, pp. 111–6.
52. P. Riboud, Y. Roux, L. Lucas, and H. Gaye: *Fachber. Huttenprax. Metall*., 1981, vol. 19, pp. 859–69.
53. T. Iida, H. Sakai, Y. Kita, and K. Shigeno: *ISIJ Int*., 2000, vol. 40, pp. S110–14.
54. K.C. Mills and S. Sridhar: *National Physical Lab*, 1992.
55. A. Shankar: Ph.D. Thesis, Royal Institute of Technology, Stockholm, 2007.
56. H.S. Ray and S. Pal: *Ironmak. Steelmak*., 2004, vol. 31, pp. 125–30.
57. X.J. Hu, Z.S. Ren, G.H. Zhang, L.J. Wang, and K.C. Chou: *Int. J. Min. Metall. Mater*., 2012, vol. 19, pp. 1088–92.
58. L. Gan and C. Lai: *Metall. Mater. Trans. B*, 2013, vol. 45B, pp. 875–88.
59. X.L. Tang, M. Guo, X.D. Wang, Z.T. Zhang, and M. Zhang: *Beijing Keji Daxue Xuebao*, 2010, vol. 32, pp. 1542–46.
60. M. Suzuki and E. Jak: *Metall. Meter. Trans. B*, 2013, vol. 44B, pp. 1451–65.
61. A.N. Grundy, H. Liu, I.H. Jung, S.A. Decterov, and A.D. Pelton: *Int. J. Mater. Res*., 2008, vol. 99, pp. 1185–94.
62. A.N. Grundy, I.H. Jung, A.D. Pelton, and S.A. Decterov: *Int. J. Mater. Res*., 2008, vol. 99, pp. 1195–209.
63. Q. Shu: *Ironmak. Steelmak*., 2015, vol. 42, pp. 641–47.
64. G.H. Zhang, K. Mills, and C. Chou: *Steel Res. Int*., 2013, vol. 84, pp. 631–7.
65. J.Frenkel: *Acta phys.-chim. URSS*., 1935, vol. 3, pp.913-38.
66. J.A. Duffy and M.D. Ingram: *J. Inorg. Nucl. Chem*., 1975, vol. 37, pp. 1203–6.
67. H Vogel: *Phys. Z*., 1921, vol. 22, pp. 645–46.
68. G.S. Fucher: *J. Am. Ceram. Soc*., 1925, vol. 8, pp. 339–55.
69. G. Tammann and W. Hesse: *Z. Anorg. Allg. Chem*., 1926, vol. 156, pp. 245–57.
70. J.N. Tiwary, S. Sarkar, B. Mishra, and U.K. Mohanty: *Emerg. Mater. Res*., 2013, vol. 2, pp. 152–162.
71. H. Ramberg: *J. Geol*., 1952, vol. 1, pp. 331–55.
72. T. Licko and V. Danek: *Phys. Chem. Glasses*, 1986, vol. 27, pp. 22–26.
73. S.G. Bratsch: *J. Chem. Educ*., 1988, vol. 65, pp. 223–35.
74. P.M. Bills: *J. Iron Steel Inst*., 1963, vol. 201, pp. 133–40.
75. G. Urbain, Y. Bottinga, and P. Richet: *Geochim. Cosmochim. Acta* , 1982, vol. 46, pp. 1061–72.
76. R.A. Lyutikov and L.M. Tsylev*: Izv. Vkad. Nauk. SSSR Otd. TSch. Nauk. Metall. Gorn. Delo*, 1963, vol. 1, p. 41.
77. T. Yasukouchi, K. Nakashima, and K. Mori: *Tetsu-to-Hagane*, 1999, vol. 85, pp. 571–7.
78. S. Tunezo and Y. Kawai: *The Research Insitute of Mineral Dressing and Metallurgy*, 1951, pp. 492–501.
79. G.H. Zhang and K.C. Chou: *ISIJ Int*., 2013, vol. 53, pp. 177–80.
80. M.J. Toplis and D.B. Dingwell: *Geochim. Cosmochim. Acta* , 2004, vol. 68, pp. 5169–88.